# Effect of Coordination Geometry on the Gas-Phase Reactivity of Four-Coordinate Divalent Metal Ion Complexes

**Marianny Y. Combariza and Richard W. Vachet***

*Department of Chemistry, University of Massachusetts, Amherst, Massachusetts 01003*

*Received: November 7, 2003; In Final Form: January 13, 2004*

The gas-phase reactions of ammonia with $M(EN\text{-}(py)_2)^{2+}$, $M(en)(phen)^{2+}$, and $M(phen)_2^{2+}$, where M is Mn(II), Fe(II), Co(II), Ni(II), Cu(II), or Zn(II), EN-$(py)_2$ is 1,6-bis(2-pyridyl)-2,5-triazahexane, en is ethylenediamine, and phen is 1,10-phenanthroline, have been studied in a quadrupole ion trap mass spectrometer. The trends in reactivity as a function of the metal are noticeably different for each complex despite the similarity of the ligand donor groups. These results indicate that coordination geometry and electronic structure have a significant impact on the gas-phase reactivity of four-coordinate metal complex ions. Specifically, for $M(EN\text{-}(py)_2)^{2+}$ the equilibrium constants for the reactions with ammonia follow the trend Mn ≈ Fe ≈ Co > Zn ≫ Cu > Ni. The trend for the equilibrium constants of the $M(en)(phen)^{2+}$ complexes is Mn ≈ Co ≫ Ni > Cu > Zn, and for the $M(phen)_2^{2+}$ complexes, the trend is Ni > Mn ≈ Fe > Co > Cu > Zn. The most notable changes in reaction equilibrium constants occur for the Ni and Zn complexes, which increase and decrease, respectively, as the ligands are changed from EN-$(py)_2$ to (en)(phen) to $(phen)_2$. Molecular orbital stabilization energy (MOSE) and density functional theory (DFT) calculations are used to explain the experimental trends. Calculations indicate that the changes in reactivity observed for the Ni complexes are a result of different complex geometries; $Ni(EN\text{-}(py)_2)^{2+}$ is a low-spin square-planar complex, and $Ni(phen)_2^{2+}$ is a high-spin tetrahedral complex. The decreased reactivity of the Zn complexes is due to the formation of a less distorted tetrahedral complex upon going from $Zn(EN\text{-}(py)_2)^{2+}$ to $Zn(phen)_2^{2+}$. In addition, calculations show that the reactivities of the Mn, Fe, and Co complexes are consistent with slightly distorted tetrahedral structures, and the reactivities of the Cu complexes indicate that the complexes of this metal are close to square planar.

## Introduction

Knowledge of the gas-phase structures of metal complexes is important for analytical, as evidenced by several reviews,[1−4] but also fundamental reasons. An enormous amount of fundamental information has been gathered about specific bond activation by metal ions as a function of electronic structure, ligand chemistry, and thermodynamic factors via gas-phase studies.[5−12] Indeed, recent experiments have drawn very direct comparisons to catalytic species involved in, for example, olefin metathesis,[13−16] C−H bond activation,[17−19] epoxidation reactions,[20,21] and alcohol oxidation reactions.[22] These investigations benefit from the ability to evaluate catalytically active species in the gas phase that are too transient to study in solution. The otherwise short lifetimes of such species in solution do not pose a problem in the high-vacuum environment of a mass spectrometer. Furthermore, intermediates or catalytically active species of interest can readily be isolated and studied without interferences from counterions, solvent, or additional complexes that are usually present in solution. Studies of metal complexes in the gas phase have also provided insight into metal ion and metal complex microsolvation.[23−27] Again, the controlled environment of a mass spectrometer allows measurements of solvation enthalpies and can provide insight into the details of the first and second solvation shells around metal ions and metal ion complexes. In all of these studies, knowing the gas-phase structure of the metal complexes of interest enhances our understanding of the underlying chemistry.

Several means of gathering gas-phase structural information for metal complexes have been developed. Often these methods rely on a synergy between experimental results and theoretical calculations to draw conclusions. Experimentally, dissociation techniques are commonly applied because mass spectrometers are very good at measuring mass changes that accompany ion dissociations. Gas-phase ion dissociations are typically induced by collisional activation or photoactivation. With collision-induced dissociation (CID), the magnitude of the mass change is used to identify functional groups in metal complexes.[28−33] Alternatively, the energetics of the dissociation process can be used to draw conclusions about metal complex structure,[34−36] especially when used in conjunction with calculations. In some photoactivation methods, the kinetics and energetics of ion dissociation provide insight into gas-phase structure,[37,38] again with help from theoretical calculations. In other photoactivation techniques, the wavelengths required to dissociate ions are measured in a manner very similar to solution-based optical spectroscopic methods.[39−46] Such photodissociation methods can provide very detailed structural information, but these methods are experimentally challenging and are usually limited to relatively small complexes.

The most readily accessible and experimentally straightforward technique for attempting to gather structural information for metal complexes in the gas phase is CID. This method, however, has some limitations. One drawback is that upon energy deposition the structure of the ion might rearrange so that the product ions are not necessarily indicative of the initial parent ion structure. For organic ions, this is often not a problem. For metal−ligand complexes in which the metal−ligand bonds

* Corresponding author. E-mail: rwvachet@chem.umass.edu. Phone: (413) 545-2733. Fax: (413) 545-4490.

10.1021/jp0373954 CCC: $27.50 
Published on Web 02/14/2004

are usually weaker than the intraligand bonds, rearrangement of the coordination structure before dissociation can possibly occur. Also, upon dissociation it is often difficult to determine if a lost fragment was originally bound to the metal or not. Consequently, we have begun to investigate another means of gathering metal-complex structural information using a more gentle approach that involves ion−molecule (I−M) reactions. I−M reactions maintain much of the simplicity of CID experiments and can often be performed on the same instrumentation used to carry out CID experiments.

Recently, we have demonstrated that I−M reactions can provide some insight into the coordination structure of metal-complex ions. These reactions can indicate the coordination number of a metal complex when the appropriate reagent gas is chosen either to react selectively with complexes of a given coordination number[47−49] or to "titrate" the open coordination sites.[50] The kinetics and thermodynamics of these reactions have also been shown to be very sensitive to the functional groups bound to the metal in the complex.[50] To further assess the sensitivity of gas-phase I−M reactions to metal-complex coordination structure, we present here a study of the reactions of four-coordinate metal-complex ions with ammonia.

## Experimental Section

**Instrumentation.** Ion−molecule reactions were performed on a modified quadrupole ion trap mass spectrometer (Bruker ESQUIRE-LC, Billerica, MA). Instrument modifications and experimental conditions have been previously described,[50] but a brief overview is provided below.

Reagent and buffer gases were introduced into the ion trap through a set of precision leak valves obtained from MDC Vacuum Products Corporation (Hayward, CA). An ion gauge was used to monitor the pressure inside the mass spectrometer. To obtain an accurate gas pressure, a calibration of the ion gauge was performed using the known deprotonation reaction rates of the $13^+$, $12^+$, and $11^+$ charge states of ubiquitin with $NH_3$ (99.99%, Matheson Tri-gas, Parsippany, NJ).[51] The correction factor obtained from the calibration was then used, together with the ion gauge sensitivity to $NH_3$, $CH_3CN$, and He,[52] to calculate the real pressures of the gases inside the mass spectrometer. He, $NH_3$, and $CH_3CN$ pressures used throughout the experiments were $(1.0 \pm 0.3) \times 10^{-4}$, $(2.0 \pm 0.1) \times 10^{-6}$ and $(3.2 \pm 0.3) \times 10^{-7}$ Torr, respectively. The vacuum system temperature was monitored and kept at $300 \pm 2$ K using a heating blanket.

Ions of interest were selected and reacted with either $NH_3$ or $CH_3CN$ for different periods of time. Reaction times and ion isolation processes were controlled using ESQUIRE-LC software. Kinetic data was obtained by monitoring the change in the intensity of the product and parent ions for up to 4000 ms. Rate constants were determined by fitting the experimental kinetic data to a series of differential equations using the KinFit program.[53] Equilibrium constants were calculated as the ratio of the forward and back rate constants or as the ratio of the product and parent ion abundances at equilibrium in cases where the fitting process failed to provide meaningful values for the back rate constants.

**Ligand and Metal-Complex Synthesis.** The synthesis of the tetradentate ligand (EN-$(py)_2$) for complex **1** in Figure 1 was described previously.[47] In short, 2-pyridinecarboxaldehyde was mixed with ethylenediamine in a 2:1 (aldehyde/ethylenediamine) ratio in anhydrous methanol. The mixture was reacted for 24 h in a Parr shaking hydrogenator under a 60-psi atmosphere of $H_2$ (99.99%, Merriam-Graves, Springfield, MA) over Pd (10% Pd on carbon). The mixture was then filtered, and the final product was recovered as a yellow oil after allowing the solvent to evaporate. Bidentate ligands ethylenediamine (en) and phenanthroline (phen), for complexes **2** and **3** in Figure 1, were purchased from Sigma-Aldrich (St. Louis, MO) and used without further purification.

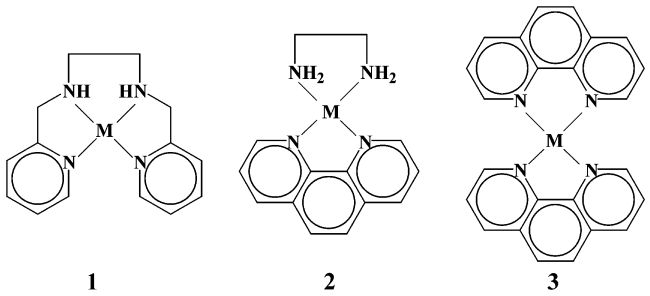


1 2 3

**Figure 1.** Complexes examined in this work: **1** = $M(EN\text{-}(py)_2)^{2+}$, **2** = $M(en)(phen)^{2+}$, and **3** = $M(phen)_2^{2+}$.

Metal complexes were prepared by mixing $MnCl_2$, $FeCl_2$, $CoCl_2$, $NiCl_2$, $CuCl_2$, or $Zn(CH_3COO)_2$ solutions with the appropriate stoichiometric amount of the ligand of interest in 100% methanol or water/methanol (50:50) to a final concentration of 50 $\mu$M. Complex ions were transferred to the gas phase by electrospray ionization using a needle voltage of about 4 kV and a flow rate of 1.0−2.0 $\mu$L/min. Typically, a capillary temperature of 150 °C and a capillary exit offset voltage of 20−30 V were used.

**Electronic Structure Calculations.** Geometry optimizations were performed on the various metal−ligand complexes using the Gaussian suite of computational chemistry programs.[54] The calculations were carried out using the B3LYP method[55−57] with a basis set containing effective core potentials (ECPs). The presence of transition-metal centers with d orbitals and generally high-spin electronic configurations makes the use of an all-electron basis set impractical for complexes of the size shown in Figure 1. ECPs were chosen instead to treat the heavy atoms in our systems. In calculations involving ECPs, only valence electrons and some outer-core electrons are considered because they are mainly responsible for bonding interactions. Electrons in the atomic core regions, presumed to be chemically inert because they are not significantly perturbed upon bonding, are represented by an ECP. Thus, the total number of electrons treated explicitly was reduced, and the calculations for systems with a large number of atoms were much more reasonable computationally. The basis set denoted as LANL2DZ in the Gaussian program was employed.[58−61] LANL2DZ contains a combination of Gaussian orbital valence basis sets and ab initio ECPs to replace the innermost core electrons for third-, fourth-, and fifth-row atoms.

## Results and Discussion

Coordinatively unsaturated divalent metal complexes readily react in the gas phase to add reagent gases. The number of reagent gas molecules added and the kinetics and thermodynamics of these reactions are found to be dependent upon the nature of the coordination sphere around the metal.[47−50,62−65] This work deals with the gas-phase reactivity of four-coordinate species formed by the complexation of metal ions from the first transition series with either one tetradentate ligand (EN-$(py)_2$) or two bidentate ligands (en and/or phen). In general, these four-coordinate complexes add one reagent molecule to become five-coordinate when reacted with $NH_3$. For some of the complexes, the addition of a second $NH_3$ molecule is also observed,

**TABLE 1: Rate and Equilibrium Constants for the Reactions of $M(EN\text{-}(py)_2)^{2+}$, $M(en)(phen)^{2+}$, and $M(phen)_2^{2+}$ Complexes with $NH_3$**

| | rate constant ($\times 10^{-11}$ cm$^3$ molecule$^{-1}$ s$^{-1}$)[a] | | | equilibrium constant ($\times 10^{9}$ atm$^{-1}$)[b] | | |
|---|---|---|---|---|---|---|
| metal | EN-(py)$_2$ | (en)(phen) | (phen)$_2$ | EN-(py)$_2$ | (en)(phen) | (phen)$_2$ |
| Mn | $17 \pm 3$ | $15 \pm 4$ | $13 \pm 4$ | $14 \pm 7$ | $30 \pm 20$[c] | $50 \pm 30$[c] |
| Fe | $12 \pm 1$ | [d] | $12 \pm 5$ | $6 \pm 0.7$ | [d] | $50 \pm 20$[c] |
| Co | $13 \pm 1$ | $7 \pm 3$ | $4.8 \pm 0.5$ | $11 \pm 4$ | $19 \pm 6$[c] | $3 \pm 1$ |
| Ni | $0.5 \pm 0.2$ | $2.2 \pm 0.7$ | $24 \pm 8$ | $0.02 \pm 0.01$ | $0.3 \pm 0.1$ | $120 \pm 40$[c] |
| Cu | $0.4 \pm 0.1$ | $0.8 \pm 0.1$ | [e] | $0.10 \pm 0.05$ | $0.10 \pm 0.02$ | [e] |
| Zn | $3 \pm 1$ | $0.8 \pm 0.1$ | $0.02 \pm 0.01$ | $4 \pm 1$ | $0.07 \pm 0.03$ | $0.005 \pm 0.002$ |

[a] These values were obtained by fitting eq 1 to the experimental data. [b] Equilibrium constants were obtained from the equation $K = k_1/k_2$, where $k_1$ and $k_2$ are the values obtained by fitting eq 1 to the experimental data. [c] The fitting for these data failed to provide a value for $k_2$, so the equilibrium constant was determined directly from the mass spectrum taken under equilibrium conditions. [d] The Fe(II) complex of (en)(phen) was difficult to generate by electrospray. [e] No significant addition of $NH_3$ to the Cu(II) complex of $(phen)_2$ was observed.

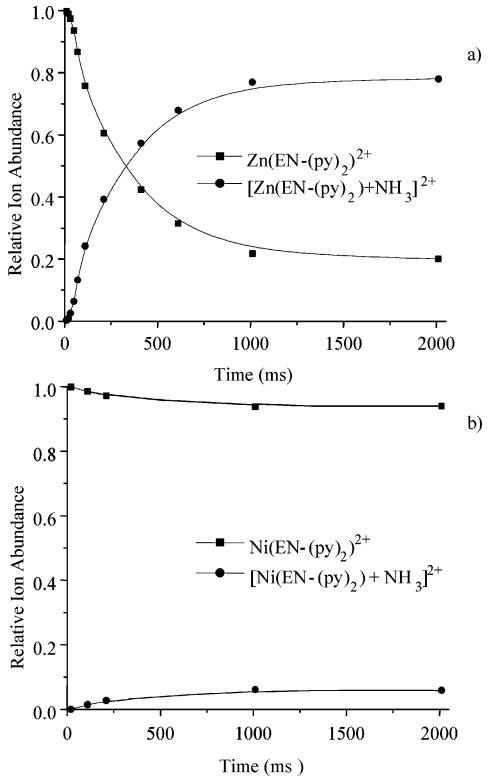


**Figure 2.** Typical kinetic plots obtained from the reactions of $NH_3$ with (a) $Zn(EN\text{-}(py)_2)^{2+}$ and (b) $Ni(EN\text{-}(py)_2)^{2+}$.

indicating the formation of a six-coordinate complex, but the abundance of this ion is generally very low. The signal corresponding to the second addition of $NH_3$ never exceeds a relative abundance of 10%, which is consistent with previous studies that demonstrated the selective reactivity of $NH_3$ with four-coordinate complexes.[47]

By monitoring the reactions of $M(EN\text{-}(py)_2)^{2+}$, $M(en)(phen)^{2+}$, and $M(phen)_2^{2+}$ complexes as a function of time, kinetic plots can be created. Figure 2 shows typical kinetic plots for the reactions of $Zn(EN\text{-}(py)_2)^{2+}$ and $Ni(EN\text{-}(py)_2)^{2+}$ with $NH_3$. From these plots, it is evident that the reactions achieve equilibrium after about 2000 ms. The establishment of an equilibrium can be confirmed by isolating the product (or parent) ion after a reaction time of 2000 ms and allowing it to react for another 2000 ms. Upon doing so, the same product/parent ion abundance ratio is reestablished. Table 1 shows that significant differences in the kinetics and thermodynamics of these reactions exist for different complexes. The kinetic behavior of the reactions follows eq 1, and the reaction rate and equilibrium constants can be determined by fitting the experimental data to this equation.

$$ML^{2+} + R \underset{k_2}{\overset{k_1}{\rightleftharpoons}} [ML + R]^{2+} \underset{k_4}{\overset{k_3}{\rightleftharpoons}} [ML + 2R]^{2+} \qquad (1)$$

The data in Table 1 clearly show that the reactivity of the four-coordinate complexes is dependent on the nature of the ligand(s) and the metal center. When EN-$(py)_2$ is the ligand, the following reactivity trend is observed as a function of the metal: Mn, Co, Fe > Zn > Cu, Ni. The trend changes slightly when the two bidentate ligands en and phen are bound to the metal (i.e., $M(en)(phen)^{2+}$ complexes) so that the observed trend is Mn, Co > Ni > Cu, Zn. An even more significant change in the reactivity is observed when two phen ligands are bound to the metal (i.e., $M(phen)_2^{2+}$ complexes) such that the trend in reactivity is Ni > Mn, Fe > Co > Cu, Zn.

**Unique Reactivity of the Ni(II) and Zn(II) Complexes.** The most notable variations in reactivity as the ligand is changed are observed for the Ni(II) and Zn(II) complexes. The equilibrium constants for the reaction of $NH_3$ with the Ni(II) complexes increase from 0.02 to 0.3 to 120 as the ligand(s) around it is-(are) changed from EN-$(py)_2$ to (en)(phen) to $(phen)_2$. In contrast, the equilibrium constants for the Zn(II) complexes decrease from 4 to 0.07 to 0.005 as the ligands are changed from EN-$(py)_2$ to (en)(phen) to $(phen)_2$. The cause of the reactivity change for the Ni(II) and Zn(II) complexes is likely due to changes in the electronic nature of each metal as the ligand is varied. Recent work showed that as the functional groups bound to a given divalent metal ion are changed from nitrogen- to sulfur- to oxygen-containing groups the gas-phase reactivity of five-coordinate metal complexes with $CH_3CN$ changed significantly.[50] The reactivity of $CH_3CN$ with the complexes in that study provided some insight into the electronic tuning of the metal by the different heteroatoms in the coordination sphere. In the present study, the ligand donor groups are not varied as much. Each ligand consists of four nitrogen donors, at least two of which are in aromatic rings. Furthermore, the reactivity of Mn, Fe, Co, and Cu complexes does not change significantly as the ligand sphere is changed. These results suggest that slight changes to the ligand donor groups are not responsible for the significant differences in reactivity observed for the Ni(II) and Zn(II) complexes.

Another possible explanation for the trends observed for the Ni(II) and Zn(II) complexes is changes in the metal electronic structure or electronic density caused by changes in the complexes' coordination geometry. Our recent results with five-coordinate complexes show that gas-phase reactivity is affected by coordination geometry[65] and that coordination geometry might be expected to affect the reactivity of four-coordinate complexes as well. In general, four-coordinate complexes adopt structures that are close to one of two ideal geometries, square planar ($D_{4h}$) or tetrahedral ($T_d$). In our experiments, upon the addition of a reagent molecule four-coordinate complexes

**TABLE 2: Molecular Orbital Stabilization Energies (MOSE) Calculated from the Angular Overlap Model for High- and Low-Spin Square Planar ($D_{4h}$), Tetrahedral ($T_d$), Square Pyramidal ($C_{4v}$), and Trigonal Bipyramidal ($D_{3h}$) Geometries, Considering Only $\sigma$ Contributions from the Ligands and $NH_3$**

| | MOSE ($e_\sigma$)[a] | | | | ΔMOSE ($e_\sigma$) | | | |
|---|---|---|---|---|---|---|---|---|
| | $D_{4h}$ | $T_d$ | $C_{4v}$ | $D_{3h}$ | $D_{4h} \rightarrow C_{4v}$ | $D_{4h} \rightarrow D_{3h}$ | $T_d \rightarrow C_{4v}$ | $T_d \rightarrow D_{3h}$ |
| | | | | High-Spin $ML_4$ to High-Spin $ML_5$ | | | | |
| Mn | −4 | −4 | −5 | −5 | −1 | −1 | −1 | −1 |
| Fe | −4 | −4 | −5 | −5 | −1 | −1 | −1 | −1 |
| Co | −4 | −4 | −5 | −5 | −1 | −1 | −1 | −1 |
| Ni | −4 | −2.67 | −5 | −3.88 | −1 | 0.125 | −2.33 | −1.21 |
| Cu | −3 | −1.33 | −3 | −2.75 | 0 | 0.25 | −1.67 | −1.42 |
| Zn | 0 | 0 | 0 | 0 | 0 | 0 | 0 | 0 |
| | | | | Low-Spin $ML_4$ to Low-Spin $ML_5$ | | | | |
| Mn | −8 | −6.67 | −10 | −8.88 | −2 | −0.88 | −3.33 | −2.21 |
| Fe | −8 | −5.33 | −10 | −7.75 | −2 | 0.25 | −4.67 | −2.42 |
| Co | −7 | −4 | −8 | −6.63 | −1 | 0.37 | −4 | −2.63 |
| Ni | −6 | −2.67 | −6 | −5.5 | 0 | 0.5 | −3.33 | −2.83 |
| Cu | −3 | −1.33 | −3 | −2.75 | 0 | 0.25 | −1.67 | −1.42 |
| Zn | 0 | 0 | 0 | 0 | 0 | 0 | 0 | 0 |
| | | | | Low-Spin $ML_4$ to High-Spin $ML_5$ | | | | |
| Mn | −8 | −6.67 | −5 | −5 | 3 | 3 | 1.67 | 1.67 |
| Fe | −8 | −5.33 | −5 | −5 | 3 | 3 | 0.33 | 0.33 |
| Co | −7 | −4 | −5 | −5 | 2 | 2 | −1 | −1 |
| Ni | −6 | −2.67 | −5 | −3.88 | 1 | 2.12 | −2.33 | −1.21 |
| Cu | −3 | −1.33 | −3 | −2.75 | 0 | 0.25 | −1.67 | −1.42 |
| Zn | 0 | 0 | 0 | 0 | 0 | 0 | 0 | 0 |
| | | | | High-Spin $ML_4$ to Low-Spin $ML_5$ | | | | |
| Mn | −4 | −4 | −10 | −8.88 | −6 | −4.88 | −6 | −4.88 |
| Fe | −4 | −4 | −10 | −7.75 | −6 | −3.75 | −6 | −3.75 |
| Co | −4 | −4 | −8 | −6.63 | −4 | −2.63 | −4 | −2.63 |
| Ni | −4 | −2.67 | −6 | −5.5 | −2 | −1.5 | −3.33 | −2.83 |
| Cu | −3 | −1.33 | −3 | −2.75 | 0 | 0.25 | −1.67 | −1.42 |
| Zn | 0 | 0 | 0 | 0 | 0 | 0 | 0 | 0 |

[a] MOSE values are given in terms of $\sigma$ overlap integrals. The values of the overlap integrals are assumed to be the same for each metal in each coordination environment.

become five-coordinate and can have trigonal-bipyramidal ($D_{3h}$) or square-pyramidal structures ($C_{4v}$). The preference for these geometric arrangements depends on the structural constraints of the ligand, the electronic nature of the donor atoms (i.e., $\sigma$ or $\pi$ donors), and the metal's number of d electrons. When the ligands are the same for a series of complexes, any differences in geometric arrangements are usually caused by the number of d electrons on the metal. In such cases, the angular overlap model (AOM)[66−69] can be used to obtain molecular orbital stabilization energies (MOSE), which can be useful as a qualitative tool in examining the effects of different geometries on d-orbital splittings.

**Angular Overlap Model Calculations.** To understand better the experimental trends observed for the four-coordinate complexes in this study, the AOM was used to calculate MOSE values for the reactant and product structures while considering all possible geometries, metal ion spin states, and $\sigma$- and $\pi$-donor contributions from the ligands. The MOSE values indicate the degree to which the d orbitals on a given metal are stabilized (or destabilized) relative to the free metal ion by a particular geometric arrangement of ligand donor groups. The degree of energetic stabilization (or destabilization) for each d orbital is typically given in terms of $\sigma$-orbital overlap integrals ($e_\sigma$), whose magnitudes are related to the $\sigma$-bonding capacity of the ligand donor groups. The difference in stabilization energy (ΔMOSE) between a product and reactant should be related to the reaction $\Delta G$ and thus the experimental equilibrium constant, assuming that the $\sigma$-orbital overlap integrals ($e_\sigma$) are similar for each metal complex. This assumption should be fairly valid given that the same ligand is bound to each metal and any systematic differences between metals cancel upon subtracting the MOSE value for the reactant from that of the product. Negative ΔMOSE values indicate a greater degree of stabilization in the product ion complex relative to the parent ion complex and thus a more favorable reaction or higher reaction equilibrium constant (i.e., $-\Delta G$).

Table 2 shows the MOSE values for ideal high- and low-spin square-planar, tetrahedral, square-pyramidal, and trigonal-bipyramidal complexes and the ΔMOSE values for all of the possible geometric transformations starting as four- and going to five-coordinate complexes. Only the $\sigma$-bonding contributions have been included in the MOSE values shown in Table 2 because including $\pi$ contributions does not lead to a better fit of the experimental data, which suggests that $\pi$ interactions have a minimal effect on the reactivity of these complexes. For all of the geometries considered, metals with between five and eight d electrons (i.e., Mn(II) through Ni(II)) can form either high- or low-spin complexes. Four-coordinate complexes of these transition metals can either be high or low spin depending on the electronic structure of the metal center and the ligand's characteristics.[70] Five-coordinate complexes of the same metals, however, are usually high spin when complexed to ligands having N-containing functional groups. Typically, ligands with weakly electronegative $\pi$ donors (e.g., P-containing functional groups) are required to obtain low-spin five-coordinate complexes.[70−72] Nonetheless, both high-spin and low-spin possibilities have been considered for the five-coordinate complexes of Mn, Fe, Co, and Ni, and the MOSE values for both cases are listed in Table 2.

The ΔMOSE values suggest that the differences in reactivity between complexes, as seen in Table 1, can be explained by differences in the geometries of the starting structures. Figure 3 shows a few combinations that help explain the experimental trends. Figure 3 and Table 2 indicate that the relatively high

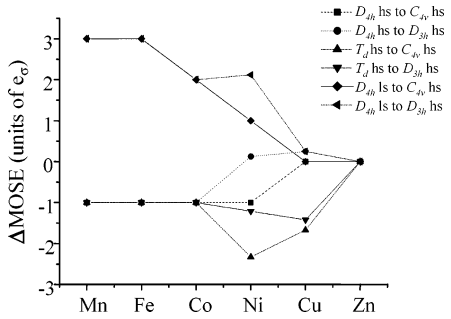


**Figure 3.** ΔMOSE values for selected transitions from four-coordinate square-planar ($D_{4h}$)/tetrahedral ($T_d$) reactants to five-coordinate trigonal-bipyramidal ($D_{3h}$)/square-pyramidal ($C_{4v}$) products.

equilibrium constants for the Mn, Fe, Co, and Zn complexes can be explained by either $D_{4h}$ or $T_d$ geometries for the reactants and either $D_{3h}$ or $C_{4v}$ geometries for the products because these transitions lead to stabilized products (i.e., negative ΔMOSE values). The reactivity of the four-coordinate Mn, Fe, and Co complexes is not explained well, though, if they are considered to be low-spin $D_{4h}$ complexes because the resulting ΔMOSE values are positive. The low equilibrium constants for Ni(EN-(py)$_2$)$^{2+}$, Ni(en)(phen)$^{2+}$, and all of the Cu complexes, however, can be explained only by $D_{4h}$ reactant geometries because transitions from this geometry lead to less-stabilized products (i.e., positive ΔMOSE values). In fact, four-coordinate complexes of $d^8$ metal ions such as Ni(II) are well known to be stable as square-planar structures.[73−75] The very high equilibrium constant for Ni(phen)$_2^{2+}$, however, can be understood by realizing that a tetrahedral Ni complex is expected to be more reactive than a square-planar Ni complex because of the greater stabilization obtained upon the addition of a fifth donor group to its coordination sphere. This result suggests that the two phen ligands enforce a geometry close to tetrahedral for Ni whereas EN-(py)$_2$ and (en)(phen) allow Ni to adopt a more square-planar geometry. Ligand-induced variations between tetrahedral and square planar in Ni(II) complexes are well known. Holm et al. reported geometric fluctuations in Ni(II) complexes as a function of the ligand's size. Basically, the introduction of bulky functional groups into ligands around Ni can enforce a high-spin tetrahedral structure whereas less-bulky functional groups on the ligands around Ni usually result in square-planar, diamagnetic geometries.[76] Evidently, the aromatic rings of the phen ligands provide enough steric bulk to force the Ni(phen)$_2^{2+}$ complex into a high-spin tetrahedral geometry, which explains its high reactivity. In contrast, the ligands in the Ni(EN-(py)$_2$)$^{2+}$ and Ni(en)(phen)$^{2+}$ complexes are less bulky and allow Ni to adopt a more favorable low-spin square-planar geometry. Furthermore, as mentioned above, five-coordinate metal complexes of first-row transition metals with amine-based ligands are usually high-spin species, and Table 2 shows that the conversion from a low-spin $D_{4h}$ complex to either a high-spin $C_{4v}$ or $D_{3h}$ complex is relatively unfavorable with positive ΔMOSE values. Thus, the reaction does not proceed very extensively.

The low equilibrium constants for Ni(EN-(py)$_2$)$^{2+}$ and Ni(en)(phen)$^{2+}$ are also the consequence of the low stability of five-coordinate Ni(II) complexes when compared to that of five-coordinate complexes of Mn(II), Fe(II), and Co(II) (Table 1). Indeed, MOSE calculations indicate that five-coordinate complexes of Ni(II) should undergo facile reagent addition because six-coordinate complexes of Ni(II) are stabilized to the same extent as six-coordinate complexes of Mn(II), Fe(II), and Co(II).[65] Given this observation, if a square-planar four-coordinate Ni(II) complex can be converted to a five-coordinate complex

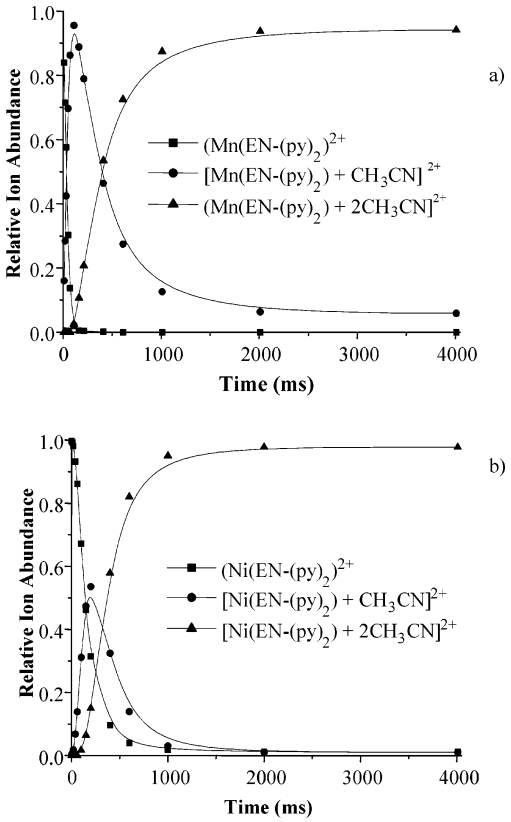


**Figure 4.** Kinetic plots for the reactions of (a) Mn(EN-(py)$_2$)$^{2+}$ and (b) Ni(EN-(py)$_2$)$^{2+}$ with $CH_3CN$.

in the gas-phase by the addition of a reagent molecule, then this five-coordinate complex should readily react to form a six-coordinate complex. Because $NH_3$ is fairly unreactive with five-coordinate complexes in the gas phase,[47] another reagent is needed to test this supposition. We observed previously that $CH_3CN$ reacted readily with five-coordinate complexes,[50] so the EN-(py)$_2$ complexes of each of the metals were reacted with this reagent gas. Figure 4 shows the kinetic plots for the reactions of Mn(EN-(py)$_2$)$^{2+}$ and Ni(EN-(py)$_2$)$^{2+}$ with $CH_3CN$. The main difference between the two plots is the relative abundance of the species [M(EN-(py)$_2$) + $CH_3CN$]$^{2+}$, which is the five-coordinate complex that is necessarily formed before the six-coordinate complex with two $CH_3CN$ molecules is formed. In the case of the Mn complex (Figure 4) and the Fe and Co complexes (data not shown), the five-coordinate complex reaches almost 100% relative abundance before it starts forming the product with two $CH_3CN$ molecules. The Ni complex, however, behaves differently. The species [Ni(EN-(py)$_2$) + $CH_3CN$]$^{2+}$ does not reach a maximum before adding the second $CH_3CN$ molecule. In fact, the Ni complex adds the second molecule of $CH_3CN$ at a faster rate than it adds the first.

The decreasing reactivity of the Zn complex upon changing the ligand is more difficult to explain using MOSE calculations because the $d^{10}$ configuration of Zn(II) prevents any ligand-field stabilization. Instead, the reduced reactivity probably has something to do with the tendency of four-coordinate Zn(II) complexes to adopt tetrahedral geometries. The EN-(py)$_2$ ligand is certainly more strained than (en)(phen) or (phen)$_2$ when trying to adopt a tetrahedral geometry. The result is that the donor atom orbitals of EN-(py)$_2$ do not overlap as effectively with Zn's d orbitals, which leads to a more electropositive Zn center that is more reactive. The two bidentate ligands in both (en)(phen) and (phen)$_2$ provide greater flexibility, and its donor

**TABLE 3: Geometric Descriptors ($\beta$, $\omega$)[a] from Optimized Structures at the DFT/LANL2DZ Level**

| | $M(EN\text{-}(py)_2)^{2+}$ | | $M(en)(phen)^{2+}$ | | $M(phen)_2^{2+}$ | |
|---|---|---|---|---|---|---|
| metal[b] | $\beta$ | $\omega$ | $\beta$ | $\omega$ | $\beta$ | $\omega$ |
| Mn | 61.0 | 76.3 | 62.1 | 73.7 | 62.8 | 72.0 |
| Fe | 61.7 | 74.7 | 61.8 | 74.5 | 59.3 | 80.2 |
| Co | 62.4 | 73.1 | 61.3 | 75.6 | 61.8 | 74.5 |
| Ni | ($S = 0$) 79.6 | 29.1 | ($S = 0$) 88.6 | 4.1 | 64.7 | 68.0 |
| Cu | 77.5 | 34.8 | 87.0 | 8.61 | 76.2 | 38.3 |
| Zn | 62.8 | 72.1 | 61.4 | 75.4 | 62.0 | 73.9 |

[a] In degrees. [b] High-spin state unless indicated otherwise. $S = {}^5/_2$ for Mn(II), $S = 2$ for Fe(II), $S = {}^3/_2$ for Co(II), $S = 1$ for Ni(II), $S = {}^1/_2$ for Cu(II), and $S = 0$ for Zn(II).

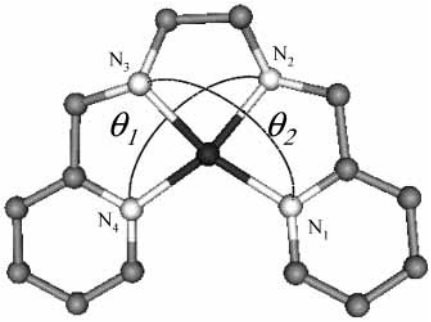


**Figure 5.** Geometry-optimized structure of $Cu(EN\text{-}(py)_2)^{2+}$ indicating the two angles used to describe $\beta$ and $\omega$. $\beta$ is the average of $\theta_1/2$ and $\theta_2/2$, and $\omega$ is defined by eq 2.

atoms can more easily orient themselves toward Zn, which leads to reduced reactivity.

**Density Functional Theory Calculations.** To further confirm these conclusions, density functional theory (DFT) calculations were also performed on each of the complexes in Figure 1. Because of the complexity of transition-metal-containing species, effective core potentials (ECP) were used to perform geometry optimizations. For complexes in which high-spin and low-spin states are possible, both were calculated. In all cases but two (i.e., $Ni(EN\text{-}(py)_2)^{2+}$ and $Ni(en)(phen)^{2+}$), the high-spin complexes were found to be considerably lower in energy. The low-spin and high-spin states of $Ni(EN\text{-}(py)_2)^{2+}$ differed by only 3.5 kJ/mol, which is within the error of the calculation, whereas the low-spin state of $Ni(en)(phen)^{2+}$ was found to be 67.3 kJ/mol lower in energy than the high-spin state. The geometric characteristics of all of the complexes calculated are displayed in Table 3. The square-planar or tetrahedral character of a four-coordinate complex can be determined from the parameters $\beta$ and $\omega$ (Figure 5). $\beta$ is defined as half of the average angle formed by the central metal atom and the two trans donor groups (i.e., $N_1-M-N_3$ and $N_2-M-N_4$ in Figure 5) and is equal to 90° for pure $D_{4h}$ geometry and 54.7° for pure $T_d$ geometry.[77] $\omega$ is the dihedral angle between the two planes that contain the central metal ion and the two cis donor groups and is equal to 0° for pure $D_{4h}$ geometry and 90° for pure $T_d$ geometry.[77] The relationship between $\beta$ and $\omega$ is given by eq 2:

$$\cos\omega = \pm\frac{1 - 3\cos^2\beta}{1 + \cos^2\beta} \qquad (2)$$

DFT calculations of $M(EN\text{-}(py)_2)^{2+}$ and $M(en)(phen)^{2+}$ show that the Ni(II) and Cu(II) complexes are the closest to square-planar geometries with the highest $\beta$ values and the lowest $\omega$ values (Table 3). The deviations from planarity in these complexes are caused mainly by ligand strain and steric interactions between the pyridine rings. The distorted square-planar structures for $Ni(EN\text{-}(py)_2)^{2+}$ and $Ni(en)(phen)^{2+}$ are consistent with their low reactivity, as suggested by the MOSE calculations. Mn, Fe, Co, and Zn complexes are closer to tetrahedral geometries, as the $\beta$ and $\omega$ values indicate. Calculations of the $M(phen)_2^{2+}$ complexes lend support to the supposition that $Ni(phen)_2^{2+}$ is tetrahedral and not square planar, which explains its increased reactivity as noted from the MOSE calculations. The hydrogen atoms on the 2 and 9 positions of the phen ligands seem to provide steric interactions that prevent Ni from adopting a preferred square-planar geometry. Interestingly, though, the Cu complex of $(phen)_2$ maintains a structure that is close to square planar. The ionic radius of Ni(II) in square-planar complexes is 0.49 Å, and for Cu(II), it is 0.57 Å.[78] Evidently, the larger radius of Cu allows it to position the phen rings further from each other so that the steric interactions between the rings are reduced and the complex can attain a square-planar structure. The low reactivity of the $Cu(phen)_2^{2+}$ complex supports this idea. The MOSE calculations indicate that square-planar Cu(II) complexes should have low reactivity and tetrahedral Cu(II) complexes should be more reactive.

## Conclusions

In summary, the results presented here indicate that I−M reactions are sensitive to the geometry of certain four-coordinate, gas-phase divalent metal-complex ions. For metals in which a different degree of stabilization is expected depending upon whether the complex is square planar or tetrahedral (e.g., Ni(II) and Cu(II)), the kinetics and thermodynamics of reagent addition can indicate the geometry of the complex. Furthermore, because four-coordinate Zn(II) complexes typically adopt tetrahedral geometries, I−M reactions may be able to provide geometric information for complexes of this metal because Zn complexes that have difficulty adopting tetrahedral geometry are likely to be more reactive than Zn complexes that can readily adopt this geometry. Currently, our results appear to be limited to simply distinguishing between the two extreme four-coordinate geometries, but future work may make it possible for I−M reactions to determine the degree of distortion in tetrahedral or square-planar structures.

Determining the gas-phase coordination geometry of metal complexes should provide some fundamentally useful information. For example, a comparison of gas-phase structures with solution-phase or solid-state structures might lend insight into the effects of solvent or crystal-packing forces on metal-complex structure. In addition, because the gas phase provides a unique environment in which short-lived (e.g., reaction intermediates) metal complexes can be studied, the ability to gather detailed coordination structure information for such complexes might provide some interesting insight into the chemical transformations that these species undergo.

**Acknowledgment.** M.Y.C thanks the Schering-Plough Research Institute for a summer research fellowship. Partial support for this work came from the Office of Naval Research under award no. N000140010796.

## References and Notes

(1) Colton, R.; D'Agostino, A.; Traeger, J. C. *Mass Spectrom. Rev.* **1995**, *14*, 79−106.

(2) Gatlin, C. L.; Tureček, F. In *Electrospray Ionization Mass Spectrometry*; Cole, R. B., Ed.; John Wiley: New York, 1997; pp 527−570.

(3) Stewart, I. I. *Spectrochim. Acta, Part B* **1999**, *54*, 1649−1695.

(4) Fisher, K. J. *Prog. Inorg. Chem.* **2001**, *50*, 343−432.

(5) *Gas-Phase Inorganic Chemistry*; Russell, D. H., Ed.; Plenum Press: New York, 1989.
(6) Armentrout, P. B.; Beauchamp, J. L. *Acc. Chem. Res.* **1989**, *22*, 315−321.
(7) Eller, K.; Schwarz, H. *Chem. Rev.* **1991**, *91*, 1121−1177.
(8) Weisshaar, J. C. *Acc. Chem. Res.* **1993**, *26*, 213-219.
(9) Eller, K. *Coord. Chem. Rev.* **1993**, *126*, 93−147.
(10) Freiser, B. S. *Acc. Chem. Res.* **1994**, *27*, 353−360.
(11) Armentrout, P. B. *Acc. Chem. Res.* **1995**, *28*, 430−436.
(12) Plattner, D. A. *Int. J. Mass Spectrom.* **2001**, *207*, 125−144.
(13) Hinderling, C.; Adlhart, P.; Chen, P. *Angew. Chem., Int. Ed.* **1998**, *37*, 2685−2689.
(14) Adlhart, C.; Volland, M. A. O.; Hofmann, P.; Chen, P. *Helv. Chim. Acta* **2000**, *83*, 3306−3311.
(15) Volland, M. A. O.; Adlhart, C.; Kiener, C. A.; Chen, P.; Hofmann, P. *Chem.*−*Eur. J.* **2001**, *7*, 4621−4632.
(16) Adlhart, C.; Chen, P. *Helv. Chim. Acta* **2003**, *86*, 941−949.
(17) Hinderling, C.; Plattner, D. A.; Chen, P. *Angew. Chem., Int. Ed. Engl.* **1997**, *36*, 243−244.
(18) Hinderling, C.; Feichtinger, D.; Plattner, D. A.; Chen, P. *J. Am. Chem. Soc.* **1997**, *119*, 10793−10804.
(19) Gerdes, G.; Chen, P. *Organometallics* **2003**, *22*, 2217−2225.
(20) Feichtinger, D.; Plattner, D. A. *Angew. Chem., Int. Ed. Engl.* **1997**, *36*, 1718−1719.
(21) Plattner, D. A.; Feichtinger, D.; El-Bahraoui, J.; Wiest, O. *Int. J. Mass Spectrom.* **2000**, *195*, 351−362.
(22) Waters, T.; O'Hair, R. A. J.; Wedd, A. G. *J. Am. Chem. Soc.* **2003**, *125*, 3384−3396.
(23) Kebarle, P. *Annu. Rev. Phys. Chem.* **1977**, *28*, 445−476.
(24) Keesee, R. G.; Castleman, A. W. *J. Phys. Chem. Ref. Data* **1986**, *15*, 1011−1071.
(25) Kebarle, P. *Int. J. Mass Spectrom.* **2000**, *200*, 313−330.
(26) Stace, A. J. *Phys. Chem. Chem. Phys.* **2001**, *3*, 1935−1941.
(27) Stace, A. J. *J. Phys. Chem. A* **2002**, *106*, 7993−8005.
(28) Hu, P.; Gross, M. L. *J. Am. Chem. Soc.* **1993**, *115*, 8821−8828.
(29) Reiter, A.; Adams, J.; Zhao, H. *J. Am. Chem. Soc.* **1994**, *116*, 7827−7838.
(30) Hopfgartner, G.; Piguet, C.; Henion, J. D. *J. Am. Soc. Mass Spectrom.* **1994**, *5*, 748−756.
(31) Hu, P.; Loo, J. A. *J. Am. Chem. Soc.* **1995**, *117*, 11314−11319.
(32) Gatlin, C. L.; Turecek, F.; Vaisar, T. *J. Am. Chem. Soc.* **1995**, *117*, 3637−3638.
(33) Alvarez, E. J.; Wu, H.-F.; Liou, C. C.; Brodbelt, J. *J. Am. Chem. Soc.* **1996**, *118*, 9131−9138.
(34) Armentrout, P. B. *Acc. Chem. Res.* **1995**, *28*, 430−436.
(35) Rodgers, M. T.; Armentrout, P. B. *Mass Spectrom. Rev.* **2000**, *19*, 215−247.
(36) Armentrout, P. B. *Int. J. Mass Spectrom.* **2003**, *227*, 289−302.
(37) Rodriguez-Cruz, S. E.; Jockusch, R. A.; Williams, E. R. *J. Am. Chem. Soc.* **1998**, *120*, 5842−5843.
(38) Stevens, S. M.; Dunbar, R. C.; Price, W. D.; Sena, M.; Watson, C. H.; Nichols, L. S.; Riveros, J. M.; Richardson, D. E.; Eyler, J. R. *J. Phys. Chem. A* **2002**, *106*, 9686−9694.
(39) Ranasinghe, Y. A.; Surjasasmita, I. B.; Freiser, B. S. In *Organometallic Ion Chemistry*; Freiser, B. S., Ed.; Kluwer Academic: Dordrecht, The Netherlands, 1996; pp 229−258.
(40) Burns, T. D.; Spence, T. G.; Mooney, M. A.; Posey, L. A. *Chem. Phys. Lett.* **1996**, *258*, 669−679.
(41) Duncan, M. A. *Annu. Rev. Phys. Chem.* **1997**, *48*, 69−93.
(42) Spence, T. G.; Burns, T. D.; Guckenberer, G. B.; Posey, L. A. *J. Phys. Chem.* **1997**, *101*, 1081−1092.
(43) Husband, J.; Aguirre, F.; Ferguson, P.; Metz, R. B. *J. Chem. Phys.* **1999**, *111*, 1433−1437.
(44) Husband, J.; Aguirre, F.; Thompson, C. J.; Laperle, C. M.; Metz, R. B. *J. Phys. Chem. A* **2000**, *104*, 2020−2025.
(45) Puskar, L.; Barran, P. E.; Wright, R. R.; Kirkwood, D. A.; Stace, A. J. *J. Chem. Phys.* **2000**, *112*, 7751−7754.
(46) Duncan, M. A. *Int. J. Mass Spectrom.* **2000**, *200*, 545−569.
(47) Vachet, R. W.; Hartman, J. R.; Callahan, J. H. *J. Mass Spectrom.* **1998**, *33*, 1209−1225.
(48) Vachet, R. W.; Callahan, J. H. *J. Mass Spectrom.* **2000**, *35*, 311−320.
(49) Vachet, R. W.; Hartman, J. R.; Gertner, J. W.; Callahan, J. H. *Int. J. Mass Spectrom.* **2001**, *204*, 101−112.
(50) Combariza, M. Y.; Vachet, R. W.; *J. Am Soc. Mass Spectrom.* **2002**, *13*, 813−825.
(51) Zhang, X.; Cassady, C. J. *J. Am. Soc. Mass Spectrom.* **1996**, *7*, 1211−1218.
(52) Bartmess, J. E.; Georgiadis, R. M. *Vacuum* **1983**, *33*, 149−153.
(53) Shen, N. Z.; Pope, R. M.; Dearden, D. V. *Int. J. Mass Spectrom.* **2000**, *196*, 639−652.
(54) Frisch, M. J.; Trucks, G. W.; Schlegel, H. B.; Scuseria, G. E.; Robb, M. A.; Cheeseman, J. R.; Zakrzewski, V. G.; Montgomery, J. A., Jr.; Stratmann, R. E.; Burant, J. C.; Dapprich, S.; Millam, J. M.; Daniels, A. D.; Kudin, K. N.; Strain, M. C.; Farkas, O.; Tomasi, J.; Barone, V.; Cossi, M.; Cammi, R.; Mennucci, B.; Pomelli, C.; Adamo, C.; Clifford, S.; Ochterski, J.; Petersson, G. A.; Ayala, P. Y.; Cui, Q.; Morokuma, K.; Malick, D. K.; Rabuck, A. D.; Raghavachari, K.; Foresman, J. B.; Cioslowski, J.; Ortiz, J. V.; Stefanov, B. B.; Liu, G.; Liashenko, A.; Piskorz, P.; Komaromi, I.; Gomperts, R.; Martin, R. L.; Fox, D. J.; Keith, T.; Al-Laham, M. A.; Peng, C. Y.; Nanayakkara, A.; Gonzalez, C.; Challacombe, M.; Gill, P. M. W.; Johnson, B. G.; Chen, W.; Wong, M. W.; Andres, J. L.; Head-Gordon, M.; Replogle, E. S.; Pople, J. A. *Gaussian 98*, revision A.3; Gaussian, Inc.: Pittsburgh, PA, 1998.
(55) Pople, J. A.; Head-Gordon, M.; Fox, D. J.; Raghavachari, K.; Curtiss, L. A. *J. Chem. Phys.* **1989**, *90*, 5622−5629.
(56) Curtiss, L. A.; Jones, C.; Trucks, G. W.; Raghavachari, K.; Pople, J. A. *J. Chem. Phys.* **1990**, *93*, 2537−2545.
(57) Becke, A. D. *J. Chem. Phys.* **1993**, *98*, 5648−5652.
(58) Dunning, T. H., Jr.; Hay, P. J. In *Modern Theoretical Chemistry*; Schaefer, H. F., III, Ed.; Plenum: New York, 1976; Vol. 3, pp 1−28.
(59) Hay, P. J.; Wadt, R. *J. Chem. Phys.* **1985**, *82*, 270−283.
(60) Hay, P. J.; Wadt, R. *J. Chem. Phys.* **1985**, *82*, 284−298.
(61) Hay, P. J.; Wadt, R. *J. Chem. Phys.* **1985**, *82*, 299−310.
(62) Hartman, J. R.; Vachet R. W.; Callahan, J. H. *Inorg. Chim. Acta* **2000**, *297*, 79−87.
(63) Hartman, J. R.; Vachet, R. W.; Pearson, W.; Wheat, R. J.; Callahan, J. H. *Inorg. Chim. Acta* **2003**, *343*, 119−132.
(64) Hartman, J. R.; Combariza, M. Y.; Vachet, R. W. *Inorg. Chim. Acta* **2004**, *357*, 51−58.
(65) Combariza, M. Y.; Fermann, J. T.; Vachet, R. W. Submitted to *Inorg. Chem.*
(66) Gerloch, M.; Woolley, R. G. *Prog. Inorg. Chem.* **1983**, *31*, 371−446.
(67) Schaffer, C. E.; Jørgensen, C. K. *Mol. Phys.* **1965**, *9*, 401.
(68) Woolley, R. G. *Mol. Phys.* **1981**, *42*, 703−720.
(69) Jørgensen, C. K. *Modern Aspects of Ligand Field Theory*; North-Holland Publishing Company: Amsterdam, 1971.
(70) Sacconi, L.; Speroni, G. P.; Morassi, R. *Inorg. Chem.* **1968**, *7*, 1521−1525.
(71) Sacconi, L. *J. Chem. Soc. A* **1970**, 248−256.
(72) Morassi, R.; Bertini, I.; Sacconi L. *Coord. Chem. Rev.* **1972**, *8*, 351−367.
(73) Weber, J. H. *Inorg. Chem.* **1967**, *6*, 258−262.
(74) Manson, W. R., III; Gray, H. R. *J. Am. Chem. Soc.* **1968**, *90*, 5721−5729.
(75) Delong, Z.; Busch, D. H. *Inorg. Chem.* **1994**, *33*, 5138−5143.
(76) Holm, R. H.; Chakravorty, A.; Theriot, L. J. *Inorg. Chem.* **1966**, *5*, 625−635.
(77) Rybak-Akimova, E. V.; Nazarenko, A. Y.; Chen., L.; Krieger, P. W.; Herrera, A. M.; Tarasov, V. V.; Robinson, P. D. *Inorg. Chim. Acta* **2001**, *324*, 1−15.
(78) Shannon, R. D. *Acta Crystallogr., Sect. A* **1976**, *32*, 751−767.